

Electronic Supplementray Information

Tuning the magnetic anisotropy in coordination nanoparticles: random distribution *versus* core-shell architecture

Yoann Prado,^{*a} Nada Dia,^a Laurent Lisnard,^{a,b} Guillaume Rogez,^c François Brisset,^a Laure Catala^{*a} and Talal Mallah^{*a}

•Materials and Instruments

-The TEM measurements have been done on a TEM Philips EM208 with 100 keV incident electrons focused on the specimen.

-Powder X-ray diffraction was performed on grown powders deposited on aluminium plate and data were collected on a Philipps Panalytical X’Pert Pro MPD powder diffractomer using CuK α radiation equipped with a fast detector.

-Energy-dispersive X-ray Spectroscopy (EDS) was carried out using an IDFix SAMx system installed on a Zeiss Supra 55 FEG-SEM. The height voltage was set at 20 kV and samples were situated at the optimal working distance. Analyses were performed on powder over a large area to get rid of topographic effects as much as possible and several analyses were done for each sample.

-Magnetic measurements were carried out with a Quantum Design MPMS-5S magnetometer working in the dc mode.

-The infra red spectra were carried out on KBr pellets containing 1% in weight of the samples. The apparatus used is a Fourier Transform Infra red Perkin Elmer 100.

•Prediction of the size of the core-shell particles

Since the core and the shell have the same structure, we can safely assume that the atomic density of the core and the core-shell particles are the same. Thus we can write:

$$N_C/V_C = N_{C-S}/V_{C-S} \quad (1)$$

where N_C and V_C are respectively the number of atoms and the volume of the core particles ; and N_{C-S} and V_{C-S} are respectively the number of atoms and the volume of the core-shell particles. The number of atoms for the core-shell particles is the sum of that of the core and the shell, thus:

$$N_{C-S} = N_C + N_S \quad (2)$$

The same relation stands for the number of moles of atoms (n), thus:

$$n_{C-S} = n_C + n_S \quad (3)$$

Equation (1) can be written in the following form:

$$V_{C-S}/V_C = (n_C + n_S)/n_C = 1 + n_S/n_C \quad (5)$$

For cubic particles of a side a , equation (5) becomes $a^3_{C-S}/a^3_C = 1 + n_S/n_C$ and hence

$$a_{C-S} = a_C (1 + n_S/n_C)^{1/3} \quad (7)$$

Equation (7) gives the relation between the size of a core-shell particle and the number of atoms of the shell that must be added n_S knowing the size of core particle a_C and its number of atoms n_C . The number of atoms in a cubic particle can be straightforwardly calculated.

•Synthesis procedures of the nanoparticles

1 is prepared by the same method already described using the negatively charged 6 nm $CsNi^{II}Cr^{III}(CN)_6$ as seeds. The preparation of **2** is similar to that of one but is carried out in two steps. The first step consists in preparing 8 nm particles of the pure $CsNi^{II}Cr^{III}(CN)_6$ and then using them as seeds to grow the 1 nm shell of the $CsCo^{II}Cr^{III}(CN)_6$ network. It is worth noting that a shell of 1 nm corresponds to two molecular layers of the bimetallic network and thus a fine control of the synthetic conditions is required. Finally, the reference nanoparticles are prepared by mixing together the three components $Cr(CN)_6^{3-}$, Co^{II} and Ni^{II} in a one pot reaction that leads to the targeted 10 nm objects **3**.

Synthesis of 6 nm $CsNi^{II}Cr^{III}(CN)_6$ particles

6 nm $CsNi^{II}Cr^{III}(CN)_6$ nanoparticles were synthesized following a previously developed method (D. Brinzei, L. Catala, N. Louvain, G. Rogez, O. Stephan, A. Gloter and T. Mallah, J. Mater. Chem., 2006, 16, 2593): an aqueous solution (100 ml) containing $NiCl_2 \cdot 6H_2O$ (0.2 mmol, 2 mM) and $CsCl$ (0.4 mmol, 4 mM) was added rapidly in an equal volume of a 2 mM aqueous solution of $K_3[Cr(CN)_6]$ (0.2 mmol) under vigorous stirring. The solution was stirred for one hour.

Synthesis of 8 nm $CsNi^{II}Cr^{III}(CN)_6$ particles

n_S/n_C indicates the ratio between the shell and core number of moles, as used in the calculation reported in the next section.

From 100 ml of the as prepared 6 nm sized $CsNi^{II}Cr^{III}(CN)_6$ nanoparticles solution, an aqueous solution (61.5 ml) of $NiCl_2 \cdot 6H_2O$ (0.123 mmol, 2 mM, $n_S/n_C = 1.23$) and $CsCl$ (0.246 mmol, 4 mM) and a 2 mM aqueous solution (61.5 ml) of $K_3[Cr(CN)_6]$ (0.123 mmol) were added in a dropwise manner (1 mL.s^{-1}) under stirring at room temperature.

Synthesis of 10 nm sized $CsNi^{II}Cr^{III}(CN)_6$ particles **1**

The 10 nm sized $CsNi^{II}Cr^{III}(CN)_6$ nanoparticles were obtained from 100 ml of the 8 nm sized nanoparticles solution adding an aqueous solution (48 ml) of $NiCl_2 \cdot 6H_2O$ (0.0953 mmol, 2 mM, $n_S/n_C = 0.953$) and $CsCl$

(0.1906 mmol, 4 mM) and a 2 mM aqueous solution (48 ml) of $K_3[Cr(CN)_6]$ (0.0953 mmol) in a dropwise manner under stirring at room temperature.

*Synthesis of 8 + 2 x 1 nm (10 nm) sized $CsNi^{II}Cr^{III}(CN)_6 @ CsCo^{II}Cr^{III}(CN)_6$ core shell particles **2***

From 100 ml of the 8 nm sized $CsNi^{II}Cr^{III}(CN)_6$ nanoparticles solution, an aqueous solution (95.3 ml) of $CoCl_2 \cdot 6H_2O$ (0.0953 mmol, 2 mM, $n_S/n_C = 0.953$) and $CsCl$ (0.1906 mmol, 4 mM) and a 2 mM aqueous solution (95.3 ml) of $K_3[Cr(CN)_6]$ (0.0953 mmol) were added in a dropwise manner under stirring at room temperature.

*Synthesis of 10 nm sized $CsNi_{0.5}^{II}Co_{0.5}^{II}Cr^{III}(CN)_6$ **3***

In the same way as the $CsNi^{II}Cr^{III}(CN)_6$ nanoparticles, an aqueous solution (100 ml) of $NiCl_2 \cdot 6H_2O$ (0.1 mmol, 1 mM), $CoCl_2 \cdot 6H_2O$ (0.1 mmol, 1 mM) and $CsCl$ (0.4 mmol, 4 mM) was added rapidly in an equal volume of a 2 mM aqueous solution of $K_3[Cr(CN)_6]$ (0.2 mmol) under vigorous stirring. The solution was stirred for one hour.

All samples were isolated according the two following procedures. An aqueous solution of nanoparticles was added to a 0.5 mM methanolic solution containing dimethyldioctadecylammonium bromide (DODABr) such as the volume ratio $MeOH : H_2O = 2.5$. The thus obtained powders of precipitated particles were used to characterize the samples in Infrared spectroscopy, X-ray diffraction, elementary analysis and transmission electronic microscopy. The magnetic studies were carried out on the nanoparticles diluted in polyvinylpyrrolidone, PVP as already reported (Y. Prado, L. Lisnard, D. Heurtaux, G. Rogez, A. Gloter, O. Stephan, N. Dia, E. Riviere, L. Catala and T. Mallah, *Chem. Commun.*, 2011, 47, 1051)

•Powder X-Ray Diffraction

The PXRD diagrams of all nanoparticles display a face centered cubic structure. The lattice constant, a , and the sizes obtained from the Scherrer formula applied to the (400) Bragg reflection are reported in the following table.

Sample	a (Å)	Size (nm)
$CsNiCr$ 8 nm	10.50	7.2
1	10.50	8.4
3	10.53	8.9
2	10.53	8.7

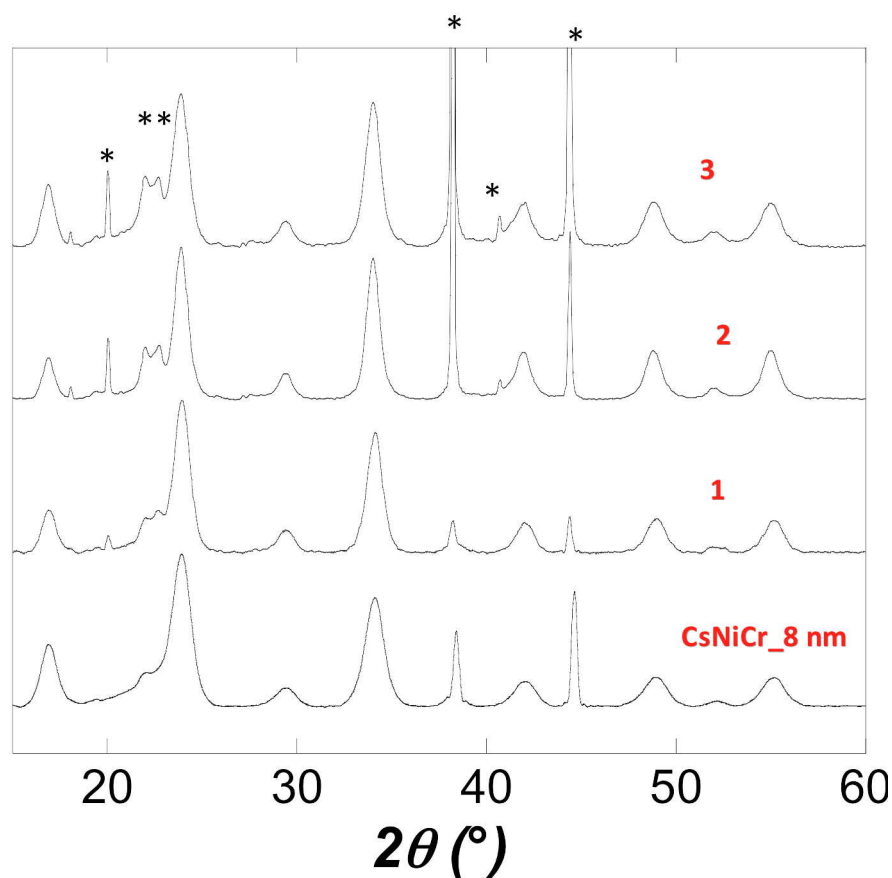


Figure S1. X-ray Powder Diffraction diagrams for the nanoparticles; ** indicates the presence of DODABr and * indicates Al from the sample holder

•Infrared spectra

The infrared spectra were made on KBr pellets (1%).

(KBr pellets, cm^{-1}): 3650 (w), 3422 (broad), 2956 (sh), 2920 (s), 2850 (s), 1616 (m), 1486 (m), 1468 (s), 1440 (w), 1419 (w), 1378 (w), 992 (w), 721 (w).

Sample	$\nu_{(M)-CN-(M')}$ (cm^{-1})	$\nu_{(M)-CN}$ (cm^{-1})	ν_{M-CN} (cm^{-1})
CsNiCr_8 nm	2172 (m)	2128 (w)	492 (s), 450 (sh), 382 (s)
1	2172 (m)	2128 (w)	492 (s), 450 (sh), 382 (s)
2	2169 (m)	2122 (w)	491 (s), 448 (sh), 379 (s), 347 (sh)
3	2169 (m)	2122 (w)	491 (s), 448 (sh), 379 (s), 347 (sh)

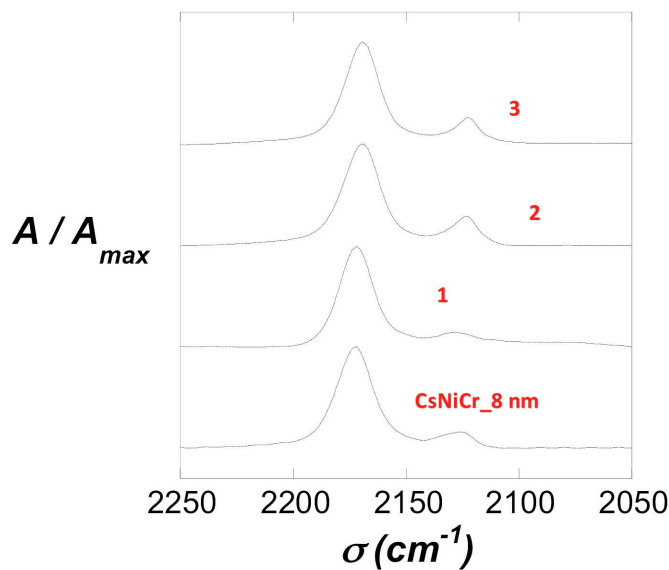


Figure S2. Infrared spectra of the nanoparticles in the 2000-2200 cm^{-1} region

•Elemental analysis

8 nm CsNiCr nanoparticles

$\text{Cs}_{0.55}\text{Ni}[\text{Cr}(\text{CN})_6]_{0.98}\{\text{DODA}\}_{0.39}\{\text{H}_2\text{O}\}_{3.7}$ ($M = 617 \text{ g.mol}^{-1}$).

Elemental analysis calcd (%) for $\text{Cs}_{0.55}\text{NiCr}_{0.98}\text{C}_{20.7}\text{N}_{6.27}\text{H}_{38.6}\text{O}_{3.7}$: Cs 11.8, Ni 9.51, Cr 8.26, C 40.3, N 14.23, H 6.3; found: Cs 11.6, Ni 9.6, Cr 8.47, C 39.9, N 13.96, H 6.2.

1 (10 nm CsNiCr nanoparticles)

$\text{Cs}_{0.53}\text{Ni}[\text{Cr}(\text{CN})_6]\{\text{DODA}\}_{0.47}\{\text{DODABr}\}_{2.8}\{\text{H}_2\text{O}\}_{5.6}$ ($M = 2464 \text{ g.mol}^{-1}$).

Elemental analysis calcd (%) for $\text{Cs}_{0.53}\text{NiCrC}_{130}\text{N}_{9.27}\text{H}_{273}\text{O}_{5.6}$: Cs 2.86, Ni 2.38, Cr 2.11, C 63.5, N 5.27, H 11.2; found: Cs 2.85, Ni 2.37, Cr 2.09, C 63.2, N 5.27, H 11.1.

2 (10 nm CsNiCr@CsCoCr core shell nanoparticles)

$\text{Cs}_{0.55}\text{Ni}_{0.52}\text{Co}_{0.48}[\text{Cr}(\text{CN})_6]_{1.03}\{\text{DODA}\}_{0.54}\{\text{DODABr}\}_{0.02}\{\text{H}_2\text{O}\}_{3.19}$ ($M = 713.2 \text{ g.mol}^{-1}$).

Elemental analysis calcd (%) for $\text{Cs}_{0.55}\text{Ni}_{0.52}\text{Co}_{0.48}\text{Cr}_{1.03}\text{C}_{27.46}\text{N}_{6.74}\text{H}_{51.2}\text{O}_{3.19}$: Cs 10.2, Ni 4.28, Co 3.96, Cr 7.5, C 46.2, N 13.2, H 7.23; found: Cs 9.96, Ni 4.16, Co 3.88, Cr 7.34, C 46.19, N 12.8, H 7.25.

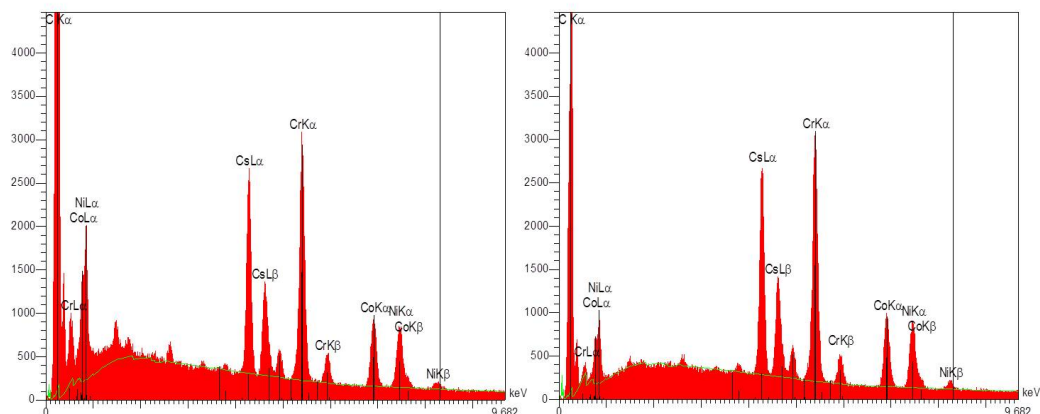
3 (10 nm CsNiCoCr nanoalloy particles)

$\text{Cs}_{0.43}\text{Ni}_{0.52}\text{Co}_{0.48}[\text{Cr}(\text{CN})_6]_{1.04}\{\text{DODA}\}_{0.69}\{\text{DODABr}\}_{0.01}\{\text{H}_2\text{O}\}_{4.43}$ ($M = 798.7 \text{ g.mol}^{-1}$).

Elemental analysis calcd (%) for $\text{Cs}_{0.43}\text{Ni}_{0.52}\text{Co}_{0.48}\text{Cr}_{1.04}\text{C}_{32.84}\text{N}_{6.94}\text{H}_{64.9}\text{O}_{4.43}$: Cs 7.15, Ni 3.82, Co 3.54, Cr 6.77, C 49.38, N 12.2, H 8.19; found: Cs 7.34, Ni 3.91, Co 3.66, Cr 6.97, C 48.15, N 12.2, H 7.95.

• Energy-dispersive X-ray spectroscopy (EDS)

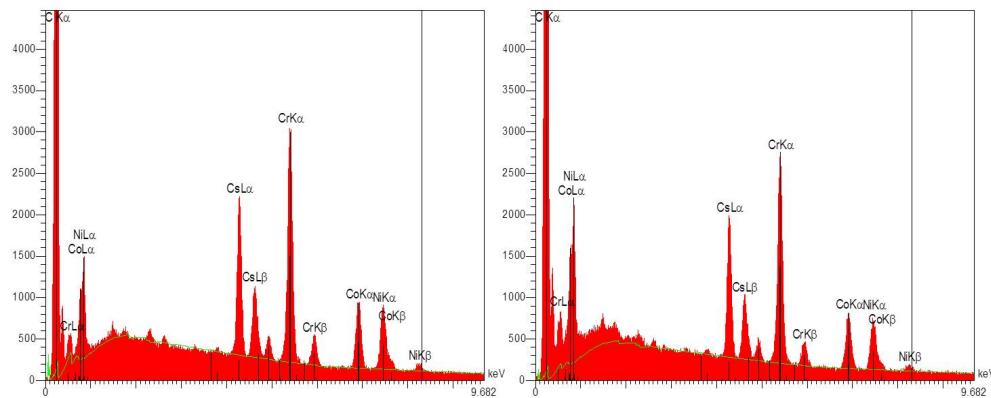
Sample 2



Elt	Line	P%	A%
C	K _α	0.00	0.00
Cr	K _α	27.83	39.55
Co	K _α	13.69	17.17
Ni	K _α	15.31	19.27
Cs	L _α	43.16	24.00
		100.00	100.00

Elt	Line	P%	A%
C	K _α	0.00	0.00
Cr	K _α	27.59	39.30
Co	K _α	13.53	17.00
Ni	K _α	15.44	19.48
Cs	L _α	43.45	24.22
		100.00	100.00

Sample 3



Elt	Line	P%	A%
C	K _α	0.00	0.00
Cr	K _α	30.38	41.43
Co	K _α	15.00	18.05
Ni	K _α	16.86	20.37
Cs	L _α	37.75	20.14
		100.00	100.00

Elt	Line	P%	A%
C	K _α	0.00	0.00
Cr	K _α	30.70	42.29
Co	K _α	14.29	17.37
Ni	K _α	15.71	19.17
Cs	L _α	39.30	21.18
		100.00	100.00

Figure S3. EDS spectra and quant tables for samples **2** and **3**.

•Zero Field Cooled / Field Cooled curves

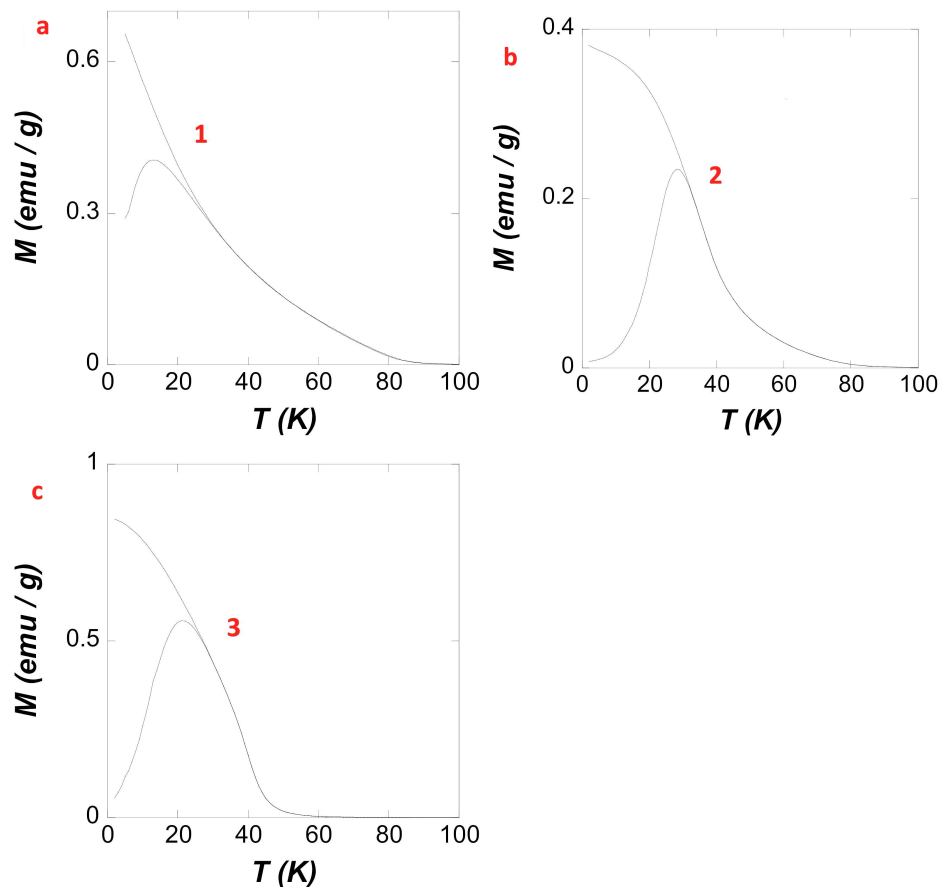


Figure S4. Field and Zero-Field Cooled Magnetization curves for **1**, **2** and **3** measured within an applied field of 30 Oe.

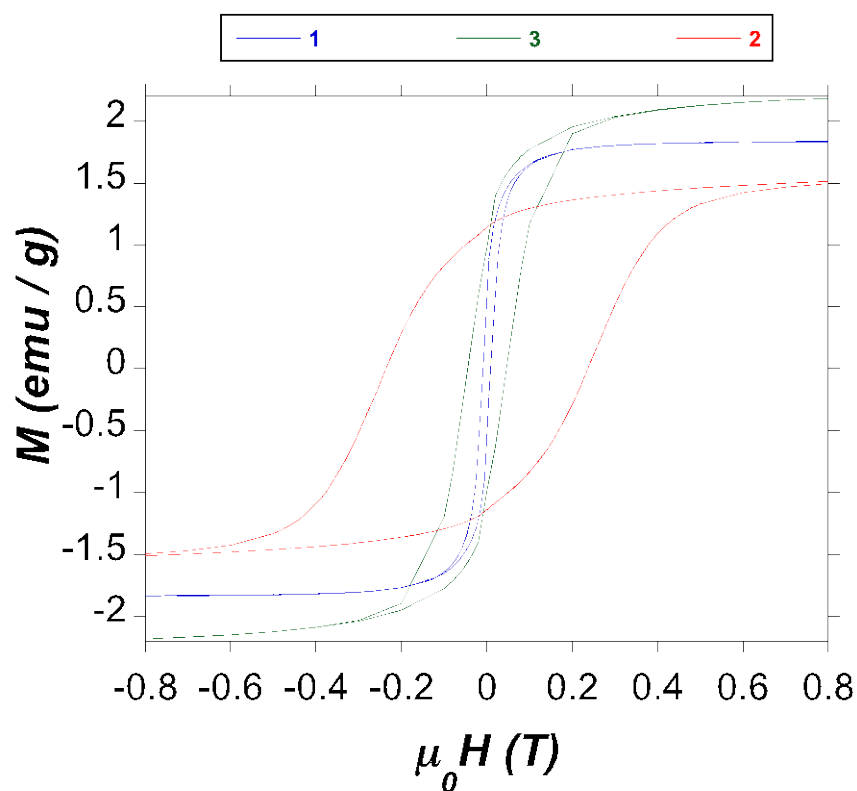


Figure S5. Hysteresis loops at $T = 2$ K for **1** (blue), **2** (red) and **3** (green)